

## Response to Reviewer #2

We sincerely appreciate Reviewer #2 for spending his/her invaluable time to give us lots of constructive, critical and helpful comments. However, it seems that the reviewer reviewed our draft not based on our final response to the reviewer but based on Authors' Comment (AC) submitted at 30<sup>th</sup> September 2019. The reason why we think like this is because the figure numbers (e.g., Fig.R8, Fig. R7) mentioned in the reviewer's final comment was not in our final response to the reviewer but in the AC. Given this special situation, all of the reviewer's comments were treated and reflected in the revised manuscript with utmost care. Our responses to individual comments are listed below.

### Major comments

**1. First of all, is the file “acp-2019-199-manuscript-version5.pdf” the final revised manuscript? It seems some of the figures are older than those in the Author's response, eg, Fig. 3 vs. Fig. R2 and Fig. 6 vs. Fig. R8.**

→ We guess “Fig. R2” and “Fig. R8” you mentioned are Fig. R1 and Fig. R2 below, respectively. In the previous revision stage, we included Fig. R1 below not in the manuscript but in the supplementary information. According to your comment, we now provide vertical profiles of cloud properties including ERA-Interim data (Fig. R1) as Fig. 3 in the manuscript (line 164-166). Fig. 6, however, is maintained in the manuscript. Here, we provide “NCD-ice” in Fig. R2 below to check whether the larger moisture transport leads to the more NCD for cloud ice, as you asked in the previous minor comment #14. The result shows that, in both models, the poleward moisture transport affects only NCD for cloud liquid (NCD-liq in Fig. R2). Therefore, in the course of the study, we focus on NCD for cloud liquid.

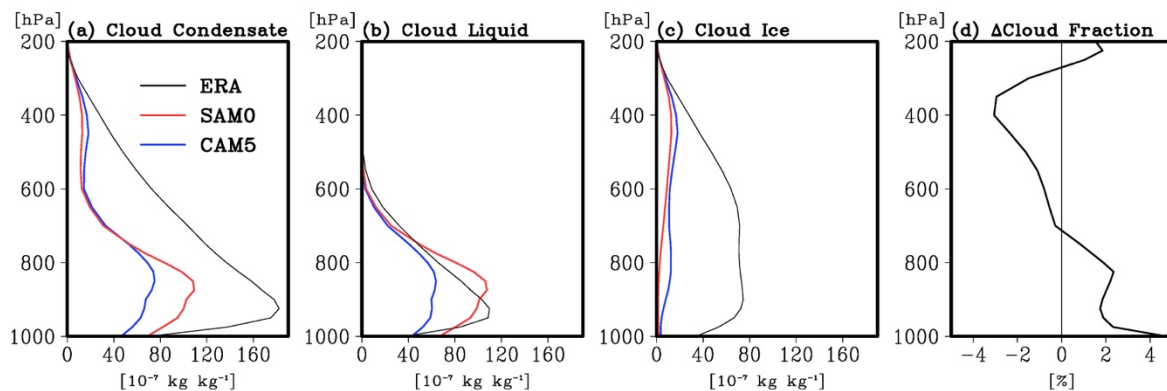


**Figure R1. Annual-mean vertical profiles of grid-mean (a) cloud condensate mass (cloud liquid + cloud**

ice), (b) cloud liquid mass, (c) cloud ice mass averaged over the Arctic area from ERA-Interim (ERA, black line), SAM0 (red lines), and CAM5 (blue lines), and (d) the difference of cloud fraction between SAM0 and CAM5.

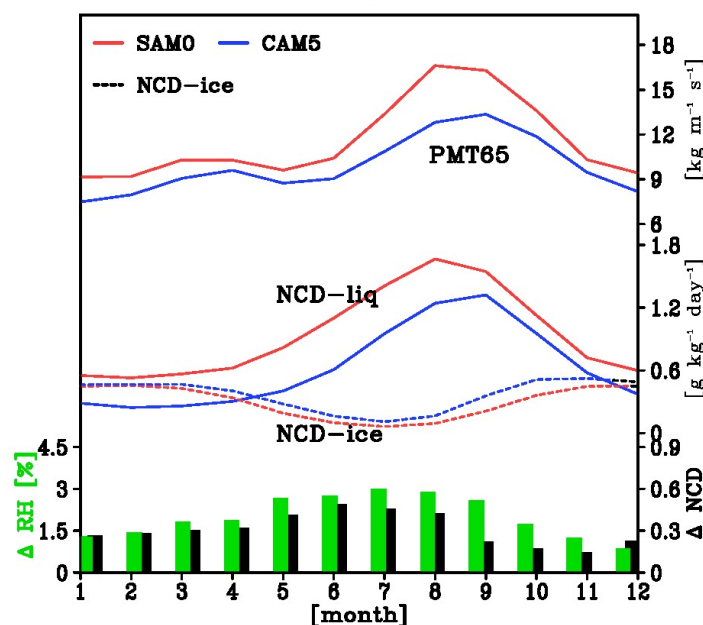


Figure R2. Annual cycles of zonal-mean poleward moisture transport (PMT65) at  $65^\circ \text{N}$ , net condensation rate of water vapor into cloud liquid (NCD-liq, center solid line), and net condensation rate of water vapor into cloud ice (NCD-ice, center dashed line) averaged over the Arctic area from SAM0 (red line) and CAM5 (blue line) and the differences of NCD-liq (black bars) and relative humidity (green bars)

2. It will also be helpful if the authors could cite the revised manuscript in the Author’s response after specific comments (or point out where in the manuscript), instead of just saying “revised in the manuscript”.  
 → We think that the reviewer reviewed our draft not based on our final “response to the reviewer” but based on “Authors’ Comment”, as mentioned above. We cited the manuscript in detail in final “response to reviewer”. In this version, we also cite the manuscript in detail.

3. To follow on my third major comment, as I worried, SAM0 reduces negative biases in poleward moisture transport yet introduces more positive biases (Fig. S5). It is not surprising that more water vapor leads to more cloud liquid condensation in the Arctic in summer. An alternative explanation for the improved cloud simulation could be that SAM0 overestimates moisture transport into the Arctic that enhances NCD and thus increases cloud liquids. Nevertheless, SAM0 still underestimates cloud fraction and liquid clouds, especially over ocean/ice (Fig. S1), indicating that enhanced moisture transports may not be a key factor for better simulations of Arctic clouds and definitely not a solution. In order to prove enhanced moisture transport is a concrete improvement, more thorough validation (eg, seasonality and pathways) against multiple datasets is needed.

→ We totally agree with your comment. As you mentioned, our study has not demonstrated that the poleward moisture transport in SAM0 is improved compared to that of CAM5. Instead, in the revised manuscript, we demonstrated that “enhanced heat and moisture transport improve Arctic climate simulations”. All of the relevant sentences are corrected in the revised manuscript (line 25-26, line 234, and line 350-351).

### **Other comments:**

#### **1. In Fig. R7, why not compare SAM0 and CAM5 against ERA-Interim directly?**

→ We guess “Fig. R7” you mentioned denotes horizontal pathway of poleward moisture transport and its convergence. This figure was provided to your major comment #3. We no longer demonstrate that poleward moisture transport of SAM0 is improved compared to that of CAM5 as we mentioned above. Please understand omitting this figure.

#### **2. Minor comment 17, since one major argument of this manuscript is that the strong correlation between moisture transports and NCD suggests a causal link, my question is relevant and within the scope of this study. (Minor comment 17: Page 9 Figure 5 a and b, the correlation seems to weaken in the recent years. Any reasons?)**

→ First of all, we are sorry for missing your question. To provide the best answer for your question, we plotted the same figure except for during recent years (1998-2014) (Fig. R3). We found that the correlation is high (correlation coefficient 0.82) even during recent years as much as during the entire period in both two models. Nevertheless, we think that the reason why the correlation seems to weaken in recent years in Fig. 7a and b is that the NCD for cloud liquid increased since 2000, unlike PMT65. One of the reasons for the increased NCD for cloud liquid may be the decline of Arctic sea ice. When the sea ice is melted, the surface moisture flux increases, which in turn can cause an increase in the Arctic water vapor source. In both models, we found that the surface moisture flux has increased over the region where sea ice melted in recent years (Fig. R4). Related research on the impact of climate change on Arctic clouds will be the subject of our future work.

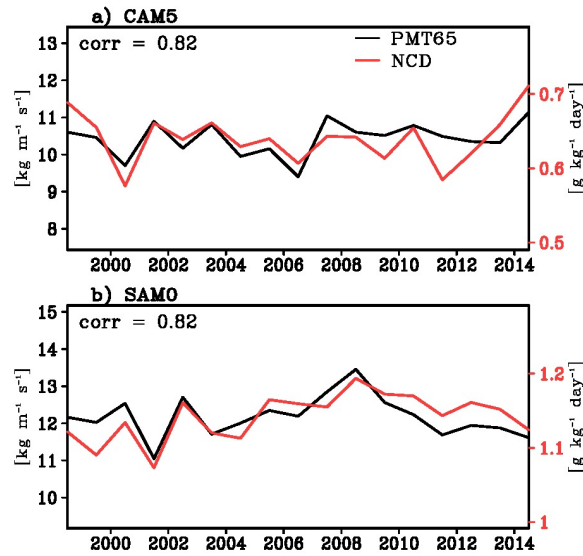


Figure R3 Interannual time series of the vertically-integrated annual-mean poleward moisture flux at 65° N (PMT65, black line) and net condensation rate of water vapor into cloud liquid (NCD, red line) averaged over the Arctic area during recent years from (a) CAM5 and (b) SAM0

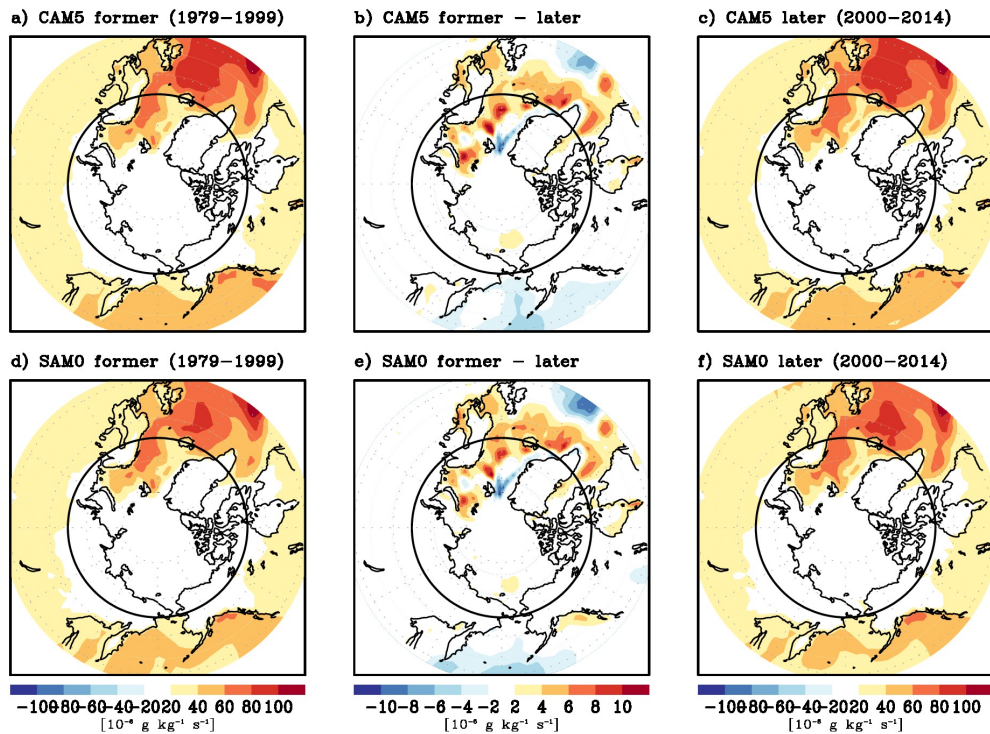


Figure R4 Surface moisture flux during former period (1979-1999) (left panel) and during later period (2000-2014) (right panel) and the difference between the two periods (center) from CAM5 (upper) and SAM0 (bottom)

## Response for Reviewer #3

We sincerely appreciate Reviewer 3 for spending his/her invaluable time to give us helpful comments. Most comments were carefully reflected in the revised manuscript. Our responses to individual comments are listed below.

**L163-164: ERA-I is not equivalent to observations. Labeling ERA-I as observations can be misleading (especially in figures). For example, ERA-I can still have large biases compared to CloudSat+CALIPSO or CERES-EBAF when it comes to downwelling shortwave surface fluxes in the Arctic (as large as  $\sim 30$  W/m<sup>2</sup>). LWP biases can be as large as  $\sim 50$  g/m<sup>2</sup> in the Norwegian and Barents Sea. I suggest the authors to replace “observations” with “reanalysis” when it’s referring to ERA-I.**

**L224: Same as above.**

→ Thank you for your kind comment. We totally agree with you and replace all of them in the revised manuscript (line 164, 165, 229, 245, and 295).

**L275: I do not understand why the authors keep showing figures of TCA, but the discussion is only relevant for LCA. Mid and high clouds can also affect TOA radiative fluxes, if they are optically thick enough, though it does not seem to be the case here. There is not a single figure showing that LCA is the dominant cloud type in the Arctic in SAM0. I suggest the authors replace TCA figures with LCA in the manuscript.**

→ We agree with your comment. We replaced TCA with LCA in Fig. 9 and the related sentences were corrected in the revised manuscript (line 290-296). However, previous studies have reported that, in summertime, Arctic mid and high clouds are optically thick enough to affect the TOA radiative flux at altitudes above 6 km (e.g. Lawson and Zuidema, 2009). Therefore we concluded to discuss not LCA but TCA for SWCF and LWCF during summertime. We maintained the TCA in Fig. 10 and replaced LCA with TCA in the description of the figure in the revised manuscript (line 307, 315, and 317).

**L400: repetitive title in reference**

→ Thank you. We corrected that in the revised manuscript.

**Figure 2: I appreciate the authors’ efforts to show ground-based observations from NSA. Since the absolute values are large for FSDS and FLDS, I suggest to plot the difference between observations and models instead of absolute values, so that the readers can see right away which months show the largest improvements.**

→ Thank you. We corrected that in the revised manuscript.

## Reference

Paul Lawson, R. and Zuidema, P.: Aircraft microphysical and surface-based radar observations of summertime arctic clouds, *J. Atmos. Sci.*, 66(12), 3505–3529, doi:10.1175/2009JAS3177.1, 2009.

# Impact of poleward heat and moisture transports on Arctic clouds and climate simulation

Eun-Hyuk Baek<sup>1</sup>, Joo-Hong Kim<sup>2</sup>, Sungsu Park<sup>3\*</sup>, Baek-Min Kim<sup>4\*</sup>, Jee-Hoon Jeong<sup>1</sup>

<sup>1</sup>Faculty of Earth System and Environmental Sciences, Chonman National University, 77 Yongbong-ro, Buk-gu Gwangju, 61186, South Korea

<sup>2</sup>Unit of Arctic Sea-Ice Prediction, Korea Polar Research Institute, 26 Songdomirae-ro, Yeosu-gu, Incheon, 21990, South Korea

<sup>3</sup>School of Earth and Environmental Sciences, Seoul National University, 1 Gwanak-ro, Gwanak-gu, Seoul, 08826, South Korea

<sup>4</sup>Department of Environmental Atmospheric Sciences, Pukyong National University, 49 Yongso-ro, Nam-gu, Busan, 48513, South Korea

*Correspondence to:* Sungsu Park (sungsup@snu.ac.kr) and Baek-Min Kim (baekmin@pknu.ac.kr)

**Abstract.** Many General Circulation Models (GCMs) have difficulty in simulating Arctic clouds and climate causing a large inter-model spread. To address this issue, two Atmospheric Model Inter-comparison Project (AMIP) simulations from the Community Atmosphere Model version 5 (CAM5) and from the Seoul National University (SNU) Atmosphere Model version 0 (SAM0) with a Unified Convection Scheme (UNICON) are employed to identify the mechanism that works on improving Arctic clouds and climate simulation. Over the Arctic, SAM0 simulates more cloud fraction and cloud liquid mass than CAM5, reducing the negative Arctic clouds biases in CAM5. The analysis of cloud water condensate rates indicates that this improvement is associated with an enhanced net condensation rate of water vapor into the liquid condensate of the Arctic low-level clouds, which in turn is driven by enhanced poleward transports of heat and moisture by mean meridional circulation and transient eddies. The reduced Arctic cloud biases lead to improved simulations of surface radiation fluxes and near-surface air temperature over the Arctic throughout the year. The association between the enhanced poleward transports of heat and moisture and more liquid clouds over the Arctic is also evident not only in both models but also in the multi-model analysis. Our study demonstrated that enhanced poleward heat and moisture transport in a model can improve simulations of Arctic clouds and climate.

Deleted: improvement of the

Deleted: be one of the key factors for better

## 1 Introduction

With increasing greenhouse gases, the Arctic has undergone the most rapid warming on Earth. During the last decade, the warming rate of the near-surface air temperature over the Arctic has been two to three times that of the entire globe (Johannessen et al., 2016; Screen and Simmonds, 2010; Serreze and Barry, 2011). This pronounced Arctic temperature amplification, some of which is forced by the positive feedbacks among various climate components (e.g., sea ice albedo feedback (Deser et al., 2000), water vapor and cloud feedback (Lu and Cai, 2009), as well as lapse-rate feedback (Pithan et al., 2014)), is also responsible for extreme weather and climate events over mid-latitude continents (Kug et al., 2015; Screen and Simmonds, 2013; Wu and Smith, 2016). Most General Circulation Models (GCMs) struggle to properly simulate the Arctic climate, suffering from the excessive cold surface temperature. The inter-GCM spread of greenhouse-induced warming is the largest over the Arctic (Boe et al., 2009; de Boer et al., 2012; Chapman and Walsh, 2007; Karlsson and Svensson, 2013). Many studies

40 reported that the GCM-simulated cold biases over the Arctic are associated with the biases of shortwave (SW) and longwave (LW) radiations at the surface, which are due to poor simulation of Arctic clouds (Barton et al., 2014; English et al., 2015; Karlsson and Svensson, 2013; Shupe and Intrieri, 2004).

Over the Arctic, many GCMs underestimate the cloud fraction (de Boer et al., 2012; Cesana and Chepfer, 2012; English et al., 2015; Kay et al., 2016) and cloud liquid mass (Cesana et al., 2015; English et al., 2014; Kay et al., 45 2016). Because the liquid-containing clouds (i.e., mixed-phase clouds) have a larger optical depth than pure ice clouds (King et al., 2004; Shupe and Intrieri, 2004), less cloud liquid mass causes weaker cloud radiative forcing in GCMs. Unlike in midlatitudes, the mixed-phase clouds over the Arctic can persist for several days (Morrison et al., 2011; Shupe et al., 2011). From a process perspective, cloud liquid in the mixed-phase clouds should be rapidly depleted into cloud ice within a few hours owing to the higher saturation vapor pressure over water compared with ice (i.e., the Wegener–Bergeron–Findeisen (WBF) mechanism) (Bergeron, 1935; Findeisen, 1938; Wegener, 1911). Therefore, to sustain cloud liquids for several days, a certain production mechanism needs to counteract the WBF depletion process. Morrison et al. (2011) reviewed various candidate production processes for cloud liquid in Arctic mixed-phase clouds, such as the compensating feedback between the formation and growth of cloud liquid droplets and ice crystals (Jiang et al., 2000; Prenni et al., 2007), in-cloud turbulence 50 generated by cloud top radiative cooling (Korolev and Field, 2008; Shupe et al., 2008), and horizontal advection by large-scale flows (Sedlar and Tjernström, 2009; Solomon et al., 2011). More recent studies also noted that ice nucleation may be important for correctly simulating Arctic mixed-phase clouds. Liu et al. (2011) demonstrated that their revised ice nucleation scheme increased cloud liquid mass in the Arctic mixed-phase stratocumulus and associated downward LW flux at the surface during the Fall 2004 Mixed-Phase Arctic Cloud Experiment (MPACE). Subsequent sensitivity studies with various ice nucleation schemes reported similar results (English et al., 2014; Xie et al., 2013). These improvements are attributed to the revised ice nucleation that decelerates the WBF depletion process in the mixed-phase clouds. Even with the cloud liquid mass increase, low-level cloud fraction still decreased in simulations, such that the biases of the radiation fluxes at the surface and the top-of-atmosphere (TOA) still remained.

65 In an attempt to determine the factors responsible for the negative biases in GCM-simulated cloud liquid mass and cloud fraction over the Arctic, this study will compare the Arctic climate simulated by the Seoul National University Atmosphere Model version 0 with a Unified Convection Scheme (SAM0-UNICON; Park, 2014a, 2014b; Park et al., 2017; Park et al., 2019) to that of the Community Atmosphere Model version 5 (CAM5; Neale et al., 2012; Park et al., 2014). By comparing two Atmospheric Model Intercomparison Project (AMIP) 70 simulations with CAM5 and SAM0-UNICON, we will show 1) the difference in cloud properties over the Arctic as simulated by SAM0-UNICON and CAM5, 2) the mechanisms of the improved clouds simulation, and 3) the influence of clouds simulation on the Arctic climate simulation. Model design and data used in this study will be described in Section 2. The results of the Arctic clouds simulation and related mechanism will be provided in Section 3.1. The impact of Arctic clouds on the Arctic climate simulation will be presented in Section 3.2. Finally, a summary and discussion will be provided in Section 4. 75

## 2 Method

### 2.1 Model and experimental design

SAM0-UNICON (Park et al., 2019), hereinafter, SAM0, for simplicity is an international GCM participating in the Coupled Model Intercomparison Project 6 (CMIP6) (Eyring et al., 2016). SAM0 is based on CAM5, however  
80 adopts the Unified Convection Scheme (UNICON) (Park, 2014a, 2014b) instead of the shallow (Park and Bretherton, 2009) and deep convection schemes (Zhang and McFarlane, 1995) of CAM5; further, it has a revised treatment of the cloud macrophysics process (Park et al., 2017). Other features, such as dynamic core, cloud macrophysics and microphysics, and PBL, etc. are exactly the same for both models. UNICON is a process-  
85 based subgrid convection parameterization scheme consisting of multiple convective updrafts, convective downdrafts, and subgrid cold pools and mesoscale organized flow without relying on any equilibrium constraints, such as convective available potential energy (CAPE) or convective inhibition (CIN) closures. UNICON simulates all dry-moist, forced-free, and shallow-deep convection within a single framework in a seamless, consistent, and unified manner (Park, 2014a, 2014b). The revised cloud macrophysics scheme diagnoses additional detrained cumulus by assuming a steady state balance between the detrainment rate of cumulus condensates and the  
90 dissipation rate of detrained condensates by entrainment mixing (Park et al., 2017). The addition of detrained cumulus substantially improves the simulation of low-level clouds and the associated cloud radiative forcing in the subtropical trade cumulus regime. Park et al. (2019) showed that the global mean climate, 20th century global warming, and El Niño and Southern Oscillation (ENSO) simulated by SAM0 are roughly similar to those of CAM5 and the Community Earth System Model version 1 (CESM1; Hurrell et al., 2013); however, SAM0  
95 substantially improves the simulations of the Madden-Julian Oscillation (MJO) (Madden and Julian, 1971), diurnal cycle of precipitation, and tropical cyclones, all of which are known to be extremely difficult to simulate in GCMs.

To evaluate the impact of SAM0 on the Arctic cloud system, we conducted five ensemble experiments of an AMIP simulation for 36 years from January 1979 to February 2015 with a horizontal resolution of 1.9° latitude x  
100 2.5° longitude and with 30 vertical layers for both CAM5 and SAM0. The climatology from the two simulations over the Arctic are then compared. The detailed settings of the AMIP simulations are identical to those described in Park et al. (2014). For a rational comparison with satellite observation data, the model cloud fraction is calculated using lidar simulator in the Cloud Feedbacks Model Intercomparison Project (CFMIP) Observation Simulator Package (COSPP) diagnostic model. A detailed description of the COSPP diagnostic model can be found  
105 in Kay et al. (2012).

### 2.2 Observational data

The observed Arctic cloud fraction and condensate phase information are obtained from the Cloud-Aerosol Lidar and Infrared Pathfinder Satellite Observations (CALIPSO)–GCM Oriented CALIPSO Cloud Product (CALIPSO–GOCCP) from June 2006 to November 2010 (Chepfer et al., 2010). The lidar beam of CALIPSO may not detect  
110 a few ice crystals underneath the optically thick stratocumulus clouds due to its attenuation and the CALIPSO–GOCCP may slightly underestimate the ice clouds in the lowest levels at midlatitudes and in polar regions (Cesana et al., 2015). Nevertheless, CALIPSO–GOCCP currently provides the best available satellite observations of polar clouds because it can detect optically thin clouds without relying on the albedo or thermal contrast (Cesana and



115 Chepfer, 2012; Kay et al., 2012). The observed TOA fluxes are obtained from the version 2.8 of the Clouds and  
Earth's Radiant Energy System (Wielicki et al., 1996) Energy Balanced and Filled data (Loeb et al., 2009)  
(CERES-EBAF) from March 2000 to February 2013. Although CERES-EBAF over the Arctic likely exceeds the  
global uncertainty particularly for clear sky retrievals due to the low albedo contrast between snow and clouds, it  
is the only available source of basin-wide TOA fluxes in the Arctic, and newer versions have advanced to  
120 distinguish clouds from underlying high-albedo sea ice and snow cover by utilizing cloud radiances from the  
collocated Moderate Resolution Imaging Spectroradiometer (MODIS) and sea ice concentration fields from the  
National Snow and Ice Data Center (NSIDC) (English et al., 2014). The climatology data of long-term ground-  
based cloud and radiation measurements from 1998 to 2010 at the North Slope of Alaska (NSA) Barrow site  
(71.38N, 156.68W) from the Atmospheric Radiation Measurement (ARM) Best Estimate (ARMBE) dataset (Xie  
et al., 2010) are used for the model evaluation. The Arctic near-surface air temperature at a 2 m height ( $T_{2m}$ ),  
125 liquid water path (LWP), and ice water path (IWP) are obtained from the European Center for Medium-Range  
Weather Forecasts (ECMWF) ERA-Interim reanalysis dataset from January 1979 to February 2015 (Dee et al.,  
2011).

### 2.3 CMIP5 models

To identify the relationship between the Arctic clouds and poleward transports of moisture and heat, we also  
130 analyzed AMIP simulations of the Coupled Model Intercomparison Project Phase 5 (CMIP5) (Taylor et al., 2012).  
We used the outputs from nine models (bcc-csm1-1-m, CanAM4, CNRM-CM5, GFDL-CM3, HadGEM2-A,  
IPSL-CM5A-MR, IPSL-CM5B-LR, MIROC5, and MPI-ESM-LR), which can be accessed from  
<http://pcmdi.llnl.gov/>. These models are selected based on the availability of the following model outputs: monthly  
low-cloud fraction calculated by CALIPSO COSP diagnostic model (variable name: clcalipso), liquid water path  
135 (variable name: clwvi), ice water path (variable name: clivi), daily meridional wind (variable name: va), air  
temperature (variable name: ta), and specific humidity (variable name: hus).

## 3 Results

### 3.1 Arctic clouds and their relationships with poleward moisture and heat transports

SAM0 reduces the negative biases of CAM5 in cloud fraction and liquid cloud simulations. Figure 1a shows the  
140 annual cycle of the total cloud fraction (TCA) averaged over the Arctic area (north of 65° N) obtained from  
CAM5, SAM0, and observation. Consistent with Kay et al. (2012) and English et al. (2014), CAM5  
underestimates the observed TCA throughout the year. The negative biases in the CAM5-simulated TCA are  
reduced in SAM0, which simulates a more realistic TCA, particularly during summer. SAM0 improves not only  
the cloud fraction but also the simulation of cloud phase characteristics. Cesana et al. (2015) proposed the height  
145 at which the ratio of cloud ice mass to total cloud condensate mass is 90 % (i.e., the phase ratio, PR90) as a useful  
indicator in assessing the model performance to simulate the cloud phase. The obtained PR90 in most GCMs is  
located at heights lower than that of the satellite observation, implying that most GCMs underestimate cloud liquid  
mass or overestimate cloud ice mass. Both CAM5 and SAM0 underestimate cloud liquid mass over the Arctic;  
however, SAM0 exhibits better estimates compared with CAM5 (Fig. 1b). Not only the biases against satellite  
150 observation, the biases against ground-based observation are also reduced in SAM0. Figure 2 shows the annual

cycle of TCA, LWP, surface downward short-wave radiation (FSDS), and surface downward long wave radiation (FLDS) from CAM5, SAM0, and the observation at barrow site. TCA in CAM5 is less than that of the observation except for July and August. LWP is also underestimated over the entire period. Accordingly, the downward shortwave flux is overestimated and the downward longwave flux is underestimated particularly in autumn and winter. Although TCA in SAM0 is overestimated in summertime compared with the observation, SAM0 reduces the bias of CAM5 during the other periods. The LWP is simulated closer to the observation than those in CAM5. Biases of the surface radiation fluxes are also reduced except during summertime.

Deleted: slightly

Deleted: and the surface radiation fluxes are also

Figure 3 shows the annual-mean vertical profiles of grid-mean cloud condensate masses and the difference of cloud fraction between SAM0 and CAM5 averaged over the Arctic area. Compared with CAM5, SAM0 simulates more cloud liquid condensate mass in the lower troposphere but slightly less cloud ice condensate mass throughout the troposphere (Fig. 3b and 3c). Thus, the total cloud condensate mass increases (decreases) in the lower troposphere (in the mid-troposphere) from CAM5 to SAM0, respectively, which is responsible for the difference in the cloud fraction (Fig. 3a and 3d). The increase in the cloud liquid condensate mass reduces its bias against the ERA-interim reanalysis. CAM5 underestimates both cloud liquid and ice condensation against the reanalysis (Supplementary S1b and S1e). SAM0, however, simulates the cloud liquid condensation close to the reanalysis, although the cloud ice condensation is underestimated as much as CAM5 (Supplementary S1c and S1f). These changes of cloud characteristics from CAM5 to SAM0 differ from previous report on the impact of revised ice nucleation scheme (English et al., 2014; Liu et al., 2011; Morrison et al., 2008), which simulated a smaller (larger) low-level (mid-level) cloud fraction. The increase (decrease) of cloud liquid (ice) mass is consistent with the increase of PR90 heights from CAM5 to SAM0 shown in Fig. 1b.

Deleted: ERA-interim data

Deleted: , S1e,

Deleted: S2

Deleted: observation

Deleted: , S1f

Deleted: S2

To understand the physical processes responsible for the increases of cloud fraction and cloud liquid mass in the lower troposphere from CAM5 to SAM0, we plotted the annual-mean vertical profiles of the grid-mean tendencies of cloud liquid and ice condensate masses averaged over the Arctic area from various physical processes (Fig. 4). Both CAM5 and SAM0 shows two main physical processes generating Arctic cloud liquid condensate the net condensation of water vapor into cloud liquid (NCD) simulated by the cloud macrophysics scheme and the convective detrainment of cloud liquid (DET). In contrast, two main depletion processes are observed: the precipitation–sedimentation fallout of cloud condensate (PRS) and WBF conversion of cloud liquid into cloud ice (WBF) simulated by the cloud microphysics scheme. For cloud ice condensate, the main sources are the net deposition of water vapor into cloud ice (NCD), WBF, and convective detrainment of cloud ice (DET), while the main sink is PRS (Fig. 4b). With the exception within the Planetary Boundary Layer (PBL) below 950 hPa, the grid-mean tendencies due to subgrid vertical transports of cloud condensates by local symmetric turbulent eddies (PBL) and nonlocal asymmetric turbulent eddies (CON) are generally smaller than other tendencies. Near the surface, the PBL scheme operates as a strong source for cloud liquid owing to downward vertical transport of cloud liquid mass from the cloud layers above (Fig. 4a).

The largest difference between CAM5 and SAM0 is observed in NCD and DET, particularly for cloud liquid. For cloud liquid, SAM0 simulates weaker DET but much stronger NCD than CAM5, such that the sum of NCD and DET simulated by SAM0 is larger than that of CAM5 with the maximum difference of approximately  $0.05 \text{ g kg}^{-1} \text{ day}^{-1}$  around the 850 hPa, where the differences of cloud liquid condensate mass and cloud fraction between CAM5 and SAM0 are also maximum (see Fig. 3b). This indicates that the increases of cloud fraction and cloud liquid condensate mass from CAM5 to SAM0 are mainly caused by an enhanced NCD for cloud liquid from

200 CAM5 to SAM0. The differences in PBL and CON between CAM5 and SAM0 are relatively small. For cloud  
ice, the overall production rate simulated by SAM0 is smaller than that of CAM5, mainly due to the decreases in  
NCD and DET slightly compensated by the increases in WBF and PRS, which leads to the decrease of cloud ice  
mass, as shown in Fig. 3c. The SAM0-simulated WBF tendency is slightly larger than that of CAM5 partly due  
to the larger cloud liquid mass in SAM0. In summary, the increases of cloud liquid mass, cloud fraction, and PR90  
205 from CAM5 to SAM0 shown in Figs. 1 and 3 (which are improvements) are mainly caused by the enhanced NCD  
for cloud liquid from CAM5 to SAM0. In accordance with the stronger NCD for liquid, the liquid cloud fraction  
also increases to satisfy the saturation equilibrium constraint for cloud liquid (see Appendix A of Park et al.  
(2014)).

The question on what physical process has caused the increase of NCD for cloud liquid from CAM5 to SAM0  
remained. In the both models, the NCD for cloud liquid is explicitly calculated by the saturation equilibrium in  
210 the cloud microphysics scheme, which indicates that more NCD for cloud liquid is produced with more water  
vapor and lower temperature (Park et al., 2014). Assuming that the Arctic region is a cylinder, the water vapor  
over the Arctic region can be increased only by two ways: convergence of meridional moisture flux and surface  
moisture flux. Because the difference of surface moisture flux between the two models is much smaller than that  
of the convergence of meridional moisture flux in Arctic region (compare Supplementary S2a with S2b), we  
215 inferred that the difference in the large-scale horizontal advection of moisture from sub-Arctic to Arctic caused  
the increase in the Arctic water vapor source. Figure 5 shows the differences of zonal-mean meridional transports  
of heat and moisture in high-latitude region and vertical profiles of water vapor (Q), air temperature (T), and  
relative humidity (RH) averaged over the Arctic area. The zonal-mean meridional flux is calculated as Eq. 1:

$$[\overline{vX}] = [\overline{v}][\overline{X}] + [\overline{v'X'}] + [\overline{v''X''}], \quad (1)$$

220 where  $X = Q$  or  $T$ ;  $v$  is the meridional velocity; the overbar and prime denote time-mean and departure from the  
time-mean, respectively; and the square bracket and asterisk denote zonal-mean and departure from the zonal-  
mean, respectively. The first term on the right-hand side is the flux by the mean meridional circulation, the second  
term is the flux by stationary eddy, and the last term is the flux by transient eddy.

In the midlatitude and subpolar regions, SAM0 simulates poleward transports of heat and moisture more than  
225 CAM5, particularly in the lower troposphere (Figs. 5a and 5e), mainly due to enhanced transports by mean  
meridional circulation and transient eddies (Figs. 5b–c and 5f–g). The difference of poleward moisture (heat)  
transport between SAM0 and CAM5 is approximately 10% (15%) of its climatology, respectively. The enhanced  
poleward transports of heat and moisture in SAM0 reduces its biases against the ERA-Interim reanalysis compared  
with CAM5. CAM5 overestimates both moisture and heat fluxes over the midlatitude region against the reanalysis  
230 but underestimates those on the periphery (around 70° N) of the Arctic circle (Supplementary S3). Although the  
positive bias over the midlatitude region still remains, SAM0 reduces the biases of CAM5 on the periphery  
(around 70° N) of the Arctic circle (Supplementary S4). In the northern hemisphere, SAM0 simulates higher  
pressure and temperature in the low-latitude region but lower pressure and temperature in the high-latitude region  
compared with CAM5, which reduces the bias of CAM5 (Supplementary S5). The circulation change in SAM0  
235 enhances the mean meridional circulation and polar jet stream over higher latitudes (Li and Wang, 2003). The  
associated strengthening of zonal mean meridional wind in the midlatitude region (see the contour lines in Figs.  
5b and 5f) enhances the poleward transports of heat and moisture near the surface. Enhanced polar jet stream (see  
the contour lines in Figs. 5c and 5g) strengthens the storm track activity on the periphery of the Arctic circle

Deleted: S3a

Deleted: S3b

Deleted: observation

Deleted: observation

Deleted: S4

Deleted: S5

Deleted: is an improvement compared with

Deleted: ERA-Interim observation

Deleted: S6

(between 60° N and 70° N) (Supplementary [S5c](#) and [S5f](#)) and increases the associated poleward transports of heat and moisture by transient eddies. Moreover, SAM0 simulates the convection more strongly than CAM5, particularly in most of the tropical ocean, which reduces bias from [the reanalysis](#) (Supplementary [S6](#)). Several previous studies have shown that enhanced convective activity in the Tropics enhances the poleward heat and moisture transport by inducing Rossby wave trains from Tropics toward the pole promoting warm and moist advection from midlatitude into the Arctic (Lee et al., 2014; Fluorny et al., 2015). As with those studies, SAM0 seems to capture Rossby wave trains emanating from Tropics better than CAM5 (Supplementary [S5c](#)) leading to enhanced poleward heat and moisture transport in SAM0.

Consequently, SAM0 simulated higher Q and T than CAM5 over the Arctic (Figs. 5d and 5h). Notably, although SAM0 has a higher temperature than CAM5 in the Arctic, RH in SAM0 is higher than CAM5, which reveals that the increase in poleward moisture transport into the Arctic is relatively larger than the increase in temperature.

This indicates that the poleward moisture transport into the Arctic is [one of dominant factors for the generation of](#) NCD for cloud liquid. Because the liquid cloud fraction is a function of grid-mean RH in both models, cloud fraction increases in the lower troposphere (i.e., below 700 hPa), as shown in Fig. 3d. In addition, warming associated with enhanced poleward heat transport and condensation heating is likely to reduce the amount of cloud ice mass from CAM5 to SAM0, as shown in Fig. 3c; hence, reducing the ice cloud fraction in the mid-troposphere (i.e., above 700 hPa) formulated as a function of cloud ice condensate mass in both models (Fig. 2d).

The relationships between the poleward moisture transport and NCD for cloud liquid are well shown in seasonal and interannual variabilities in both models (Figs. 6 and 7). SAM0 simulates more poleward moisture transport into the Arctic than CAM5 throughout the year (Fig. 6). In both models, the poleward moisture transports at 65° N are the largest from summer to autumn, and the associated NCD for cloud liquid averaged over the Arctic region nearly agree with the poleward moisture transport. The seasonal variability of NCD difference for cloud liquid is almost coincident with that of RH, which explains the increase in the Arctic liquid cloud fraction from May to September as shown in Fig. 1. The interannual variations of the poleward moisture transport and NCD for cloud liquid in each model are also highly correlated (Figs. 7a and 7b), with the correlation coefficients of 0.84 and 0.81 for CAM5 and SAM0, respectively. In addition, in almost all years, SAM0 simulates more poleward moisture flux and higher NCD for cloud liquid over the Arctic than CAM5, and the inter-model differences of these variables are also highly correlated (Fig. 7c). In summary, the strengthened poleward moisture transport increases NCD for cloud liquid, cloud liquid mass, and cloud fraction from CAM5 to SAM0.

The close association between the Arctic cloudiness and poleward transports of heat and moisture, as shown from the analysis of CAM5 and SAM0 simulations, also exist in other climate models. Figure 8 shows the scatter plots between the annual mean meridional transports of heat and moisture at 65° N and Arctic cloudiness and the LWP ratio (i.e., the ratio of LWP to total condensate water path,  $LWP/(LWP+IWP)$ ) obtained from the analysis of various AMIP simulations of CMIP5 models. Wide inter-model spread exists in the TCA, low cloud fraction (LCA, defined as those with tops between the surface and 700 hPa), LWP ratio, and poleward transports of heat and moisture. Except for a few outliers (e.g., bcc-csm1-1-m and MPI-ESM-LR), there is a clear inter-model proportional relationship between the meridional moisture transport and TCA and LCA (Fig. 8a and 8b). All models simulate consistently positive poleward moisture transport. However, some models simulate equatorward heat transport at 65° N and the corresponding LWP ratio over the Arctic tends to be smaller than those from the models with poleward heat transport (Fig. 8c). The models with strong poleward moisture transport tend to have

Deleted: S6c

Deleted: S6f

Deleted: observation

Deleted: S7

Deleted: S5f

Deleted: a

Deleted: factor

295 strong poleward heat transport as well. The inter-model analysis supports our conclusion that poleward moisture and heat transport is one of the key factors controlling LCA and LWP in the Arctic.

### 3.2 Impact of Arctic clouds on the Arctic climate

300 Clouds play a critical role in the surface radiative balance as a climate regulator in the Arctic region. Figure 9 shows biases of LCA, upward LW radiation flux at the top of the atmosphere (TOA) (FLUT), and  $T_{2m}$  during wintertime obtained from CAM5 and SAM0. As shown, CAM5 suffers from the negative biases of LCA, FLUT, and  $T_{2m}$  during December-January-February (DJF) (Fig. 9, left panel). In the Arctic during winter, less LCA in CAM5 reduces FLUT over the land and the sea-ice region in the lower troposphere because the temperature in the cloudy layer is higher than that at the surface (i.e., temperature inversion). Less LCA also reduces downward LW radiation at the surface (FLDS), which leads to colder near-surface air than the reanalysis, resulting in  
305 enhancement of the temperature inversion. Compared with CAM5, SAM0 simulates more LCA, FLUT, and  $T_{2m}$  over the whole Arctic (Fig. 9, center panel), such that their negative biases in CAM5 are alleviated in SAM0 (Fig. 9, right panel). Over the ocean where temperature inversion does not exist, more LCA in SAM0 results in more FLUT than CAM5 (Fig. 9e). SAM0 also simulates stronger FLDS than CAM5 over the entire Arctic, as expected (not shown).

310 Not only the biases during DJF, summertime biases of TCA, shortwave cloud radiative forcing at TOA (SWCF), and  $T_{2m}$  are also reduced from CAM5 to SAM0 (Fig. 10). In most Arctic areas except for some portions of the northern continents, CAM5 has the negative biases of TCA during June-July-August (JJA) (Fig. 10a). SAM0 simulates more TCA than CAM5 (Fig. 10b), such that most of the negative TCA biases in CAM5 over the Arctic sea ice and open ocean areas disappear (Fig. 10c). In the Arctic during summertime, cloudiness has the opposite effect on SWCF and LWCF (Supplementary S7); thus, we need to examine the two radiations at the surface to find the impact of the Arctic cloud to Arctic climate. With more TCA than CAM5, SAM0 simulates more net LW radiation at the surface (FLNS, Fig. 11b). Owing to the high albedo of underlying sea ice and snow in the vicinity of the Arctic pole, the net SW radiation at the surface (FSNS) does not change much there; however, FSNS decreases substantially in the surrounding regions of the Arctic pole (Fig. 11a). Overall, the increase of FLNS dominates over the decrease of FSNS in the Arctic pole, while the opposite is true in the surrounding regions (Fig. 11b and 11c). The associated increase of  $T_{2m}$  from CAM5 to SAM0 in the Arctic pole (Fig. 10h) decreases snow depth and surface albedo, while the opposite increases of snow depth and surface albedo occur in the surrounding continental area (Fig. 11d and 11e). The enhanced SWCF cooling near the Arctic pole in SAM0 (Fig. 10e) is the combined results of the increased TCA and decreased snow depth and surface albedo. If the Arctic sea ice fraction is allowed to change in response to the changes of overlying atmospheric conditions (e.g., coupled simulation), SAM0 is likely to simulate less sea ice fraction than CAM5 due to more TCA and warmer near-surface air temperature, which can be further accelerated by the positive surface albedo feedback (Holland and Bitz, 2003). In fact, Park et al. (2019) found that SAM0 simulates less sea ice fraction than the Community Earth System Model version 1 (CESM1, a coupled model of CAM5, Hurrell et al., 2013) over the Arctic in the 20th century  
325 coupled simulation.  
330

Deleted: TCA

Deleted: TCA

Deleted: observation

Deleted: TCA

Deleted: (mainly LCA)

Deleted: S8

Deleted: LCA

Deleted: LCA

Deleted: LCA

#### 4. Summary and Discussion

Many GCMs suffer from the cold bias over the Arctic, which has been speculated to be caused by radiation biases associated with underestimated cloud fraction and cloud liquid mass over the Arctic. To address this issue, we compared various aspects of the Arctic clouds and climate in two different AMIP simulations generated by CAM5 and SAM0.

Similar to other GCMs and previous studies, CAM5 underestimates cloud fraction and cloud liquid mass in the Arctic lower troposphere throughout the year. SAM0 alleviates these problems, although biases still persist. Our analysis showed that this improvement in the Arctic cloud simulation with SAM0 is mainly due to stronger NCD for cloud liquid, which in turn, was due to enhanced poleward transports of heat and moisture by mean meridional circulation and transient eddies. A new unified convection scheme (UNICON) in SAM0 strengthens and shifts poleward the zonal mean meridional circulation, polar jet stream, and associated synoptic storm activity on the periphery of the Arctic circle. The proportional relationship between the Arctic cloudiness and meridional transports of heat and moisture in CAM5 and SAM0 also exists not only in both models but also in a set of CMIP5 models. In association with the deficient simulations of cloud fraction and cloud liquid mass, CAM5 suffers from the negative bias of near-surface air temperature throughout the year. With more cloud fraction and cloud liquid mass, SAM0 also alleviates the cold temperature biases in the Arctic mainly by enhancing the downward LW radiation at the surface, which is consistent with the hypotheses suggested by previous studies (Barton et al., 2014; Chan and Comiso, 2013; Klocke et al., 2011; Pithan and Mauritsen, 2014; Walsh and Chapman, 1998). Our study indicates that the enhanced poleward heat and moisture transport in a model can improve simulations of Arctic clouds and climate.

Further study is in progress to investigate this hypothesis using fully coupled model. The authors are also continuously working to further reduce the remaining biases of Arctic clouds and climate by controlling convective activity simulated by UNICON and incorporating an improved ice nucleation scheme as suggested by previous studies.

Deleted: persists

Deleted: improvement of

Deleted: be one of the key factors for better

#### **Author Contributions**

370 E.-H. Baek performed the overall numerical experiments and analysis. S. Park developed and provided SAM0 and CAM5, and helped to analyze the simulation results. B.-M. Kim designed the project and helped to analyze the simulation results and the CMIP5 models. All authors contributed to conducting analyses.

#### **Competing interests**

The authors declare that they have no conflict of interest.

#### **375 Acknowledgments**

This work was supported by the Korea Polar Research Institute project titled ‘Development and Application of the Korea Polar Prediction System (KPOPS) for Climate Change and Disastrous Weather Events (PE19130)’ and the project titled ‘Korea-Arctic Ocean Observing System (K-AOOS), KOPRI, 20160245’, funded by the MOF, Korea. S. Park is supported by the Creative-Pioneering Researchers Program through the Seoul National

380 University (SNU) (grant number 3345-20180015). B.-M. Kim is supported by the Korea Meteorological Administration Research and Development Program (grant number KMI2018-03810)

## References

- Barton, N. P., Klein, S. A. and Boyle, J. S.: On the Contribution of Longwave Radiation to Global Climate Model Biases in Arctic Lower Tropospheric Stability, *J. Clim.*, 27, 7250–7269, doi:10.1175/JCLI-D-14-00126.1, 2014.
- 385 Bergeron, T.: *Proces Verbaux de l'Association de Meteorologie* (ed. Duport, P.), International Union of Geodesy and Geophysics., 1935.
- Boe, J., Hall, A. and Qu, X.: Current GCMs' Unrealistic Negative Feedback in the Arctic, *J. Clim.*, 22(17), 4682–4695, doi:10.1175/2009JCLI2885.1, 2009.
- 390 de Boer, G., Chapman, W. L., Kay, J. E., Medeiros, B., Shupe, M. D., Vavrus, S. and Walsh, J. E.: A Characterization of the Present-Day Arctic Atmosphere in CCSM4, *J. Clim.*, 25, 2676–2695, doi:10.1175/JCLI-D-11-00228.1, 2012.
- Cesana, G. and Chepfer, H.: How well do climate models simulate cloud vertical structure? A comparison between CALIPSO-GOCCP satellite observations and CMIP5 models, *Geophys. Res. Lett.*, 39(20), 1–6, doi:10.1029/2012GL053153, 2012.
- 395 Cesana, G., Waliser, D. E., Jiang, X. and Li, J.-L. F.: Multi-model evaluation of cloud phase transition using satellite and reanalysis data, *J. Geophys. Res. Atmos.*, (JUNE), n/a-n/a, doi:10.1002/2014JD022932, 2015.
- Chan, M. A. and Comiso, J. C.: Arctic cloud characteristics as derived from MODIS, CALIPSO, and cloudsat, *J. Clim.*, 26(10), 3285–3306, doi:10.1175/JCLI-D-12-00204.1, 2013.
- 400 Chapman, W. L. and Walsh, J. E.: Simulations of Arctic temperature and pressure by global coupled models, *J. Clim.*, 20(4), 609–632, doi:10.1175/JCLI4026.1, 2007.
- Chepfer, H., Bony, S., Winker, D., Cesana, G., Dufresne, J. L., Minnis, P., Stubenrauch, C. J. and Zeng, S.: The GCM-oriented CALIPSO cloud product (CALIPSO-GOCCP), *J. Geophys. Res. Atmos.*, 115(5), 1–13, doi:10.1029/2009JD012251, 2010.
- 405 Dee, D. P., Uppala, S. M., Simmons, A. J., Berrisford, P., Poli, P., Kobayashi, S., Andrae, U., Balmaseda, M. A., Balsamo, G., Bauer, P., Bechtold, P., Beljaars, A. C. M., van de Berg, L., Bidlot, J., Bormann, N., Delsol, C., Dragani, R., Fuentes, M., Geer, A. J., Haimberger, L., Healy, S. B., Hersbach, H., H??lm, E. V., Isaksen, I., K??llberg, P., K??hler, M., Matricardi, M., McNally, A. P., Monge-Sanz, B. M., Morcrette, J. J., Park, B. K., Peubey, C., de Rosnay, P., Tavolato, C., Th??paut, J. N. and Vitart, F.: The ERA-Interim reanalysis: Configuration and performance of the data assimilation system, *Q. J. R. Meteorol. Soc.*, 137(656), 553–597, doi:10.1002/qj.828, 2011.
- 410 Deser, C., Walsh, J. E. and Timlin, M. S.: Arctic Sea Ice Variability in the Context of Recent Atmospheric Circulation Trends, *J. Clim.*, 13, 617–633, 2000.
- English, J. M., Kay, J. E., Gettelman, A., Liu, X., Wang, Y., Zhang, Y. and Chepfer, H.: Contributions of clouds, surface albedos, and mixed-phase ice nucleation schemes to Arctic radiation biases in CAM5, *J. Clim.*, 27(13), 5174–5197, doi:10.1175/JCLI-D-13-00608.1, 2014.
- 415 English, J. M., Gettelman, A. and Henderson, G. R.: Arctic radiative fluxes: Present-day biases and future projections in CMIP5 models, *J. Clim.*, 28(15), 6019–6038, doi:10.1175/JCLI-D-14-00801.1, 2015.
- Eyring, V., Bony, S., Meehl, G. A., Senior, C. A., Stevens, B., Stouffer, R. J. and Taylor, K. E.: Overview of the Coupled Model Intercomparison Project Phase 6 (CMIP6) experimental design and organization, *Geosci. Model Dev.*, 9(5), 1937–1958, doi:10.5194/gmd-9-1937-2016, 2016.
- 420



- Findeisen, W.: Kolloid-Meteorologische, 2nd ed., Am. Meteorol. Soc., Boston, Mass., 1938.
- Holland, M. M. and Bitz, C. M.: Polar amplification of climate change in coupled models, *Clim. Dyn.*, 21(3–4), 221–232, doi:10.1007/s00382-003-0332-6, 2003.
- 425 Flournoy, M. D., Feldstein, S. B., Lee, S. and Clothiaux, E. E.: Exploring the Tropically Excited Arctic Warming mechanism with station data: Links between tropical convection and Arctic downward infrared radiation, *J. Atmos. Sci.*, 73(3), 1143–1158, doi:10.1175/JAS-D-14-0271.1, 2016.
- Hurrell, J. W., Holland, M. M., Gent, P. R., Ghan, S., Kay, J. E., Kushner, P. J., Lamarque, J. F., Large, W. G., Lawrence, D., Lindsay, K., Lipscomb, W. H., Long, M. C., Mahowald, N., Marsh, D. R., Neale, R. B., Rasch, P., Vavrus, S., Vertenstein, M., Bader, D., Collins, W. D., Hack, J. J., Kiehl, J. and Marshall, S.: The community earth system model: A framework for collaborative research, *Bull. Am. Meteorol. Soc.*, 94(9), 1339–1360, doi:10.1175/BAMS-D-12-00121.1, 2013.
- 430 Jiang, H., Cotton, W. R., Pinto, J. O., Curry, J. A. and Weissbluth, M. J.: Cloud Resolving Simulations of Mixed-Phase Arctic Stratus Observed during BASE: Sensitivity to Concentration of Ice Crystals and Large-Scale Heat and Moisture Advection, *J. Atmos. Sci.*, 57(13), 2105–2117, doi:10.1175/1520-0469(2000)057<2105:CRSOMP>2.0.CO;2, 2000.
- 435 Johannessen, O. M., Kuzmina, S. I., Bobylev, L. P., Martin, W., Johannessen, O. M., Kuzmina, S. I. and Bobylev, L. P.: Tellus A : Dynamic Meteorology and Oceanography Surface air temperature variability and trends in the Arctic : new amplification assessment and regionalization, 0870(May), doi:10.3402/tellusa.v68.28234, 2016.
- 440 Karlsson, J. and Svensson, G.: Consequences of poor representation of Arctic sea-ice albedo and cloud-radiation interactions in the CMIP5 model ensemble, *Geophys. Res. Lett.*, 40(16), 4374–4379, doi:10.1002/grl.50768, 2013.
- Kay, J. E., Hillman, B. R., Klein, S. A., Zhang, Y., Medeiros, B., Pincus, R., Gettelman, A., Eaton, B., Boyle, J., Marchand, R. and Ackerman, T. P.: Exposing global cloud biases in the Community Atmosphere Model (CAM) using satellite observations and their corresponding instrument simulators, *J. Clim.*, 25(15), 5190–5207, doi:10.1175/JCLI-D-11-00469.1, 2012.
- 445 Kay, J. E., Bourdages, L., Miller, N. B., Morrison, A., Yettella, V., Chepfer, H. and Eaton, B.: Evaluating and improving cloud phase in the Community Atmosphere Model version 5 using spaceborne lidar observations, *J. Geophys. Res. Atmos.*, 121(8), 4162–4176, doi:10.1002/2015JD024699, 2016.
- 450 King, M. D., Platnick, S., Yang, P., Arnold, G. T., Gray, M. A., Riedi, J. C., Ackerman, S. A. and Liou, K.-N.: Remote Sensing of Liquid Water and Ice Cloud Optical Thickness and Effective Radius in the Arctic : Application of Airborne Multispectral MAS Data, *J. Atmos. Ocean. Technol.*, 21, 857–875, 2004.
- Klocke, D., Pincus, R. and Quaas, J.: On constraining estimates of climate sensitivity with present-day observations through model weighting, *J. Clim.*, 24(23), 6092–6099, doi:10.1175/2011JCLI4193.1, 2011.
- 455 Korolev, A. and Field, P. R.: The Effect of Dynamics on Mixed-Phase Clouds: Theoretical Considerations, *J. Atmos. Sci.*, 65(1), 66–86, doi:10.1175/2007JAS2355.1, 2008.
- Kug, J.-S., Jeong, J.-H., Jang, Y.-S., Kim, B.-M., Folland, C. K., Min, S.-K. and Son, S.-W.: Two distinct influences of Arctic warming on cold winters over North America and East Asia, *Nat. Geosci.*, 8(10), 759–762, doi:10.1038/ngeo2517, 2015.
- 460

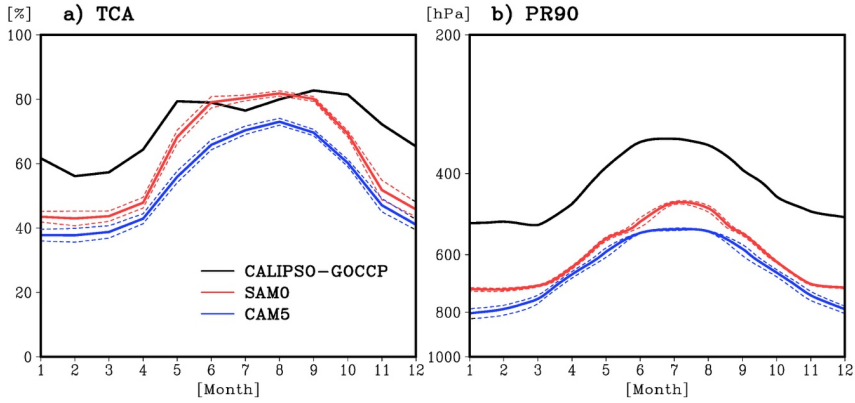
**Deleted:** regionalisation Surface air temperature variability and trends in the Arctic : new amplification assessment and regionalisation

- 465 Lee, S. and Yoo, C.: On the causal relationship between poleward heat flux and the equator-to-pole temperature gradient: A cautionary tale, *J. Clim.*, 27(17), 6519–6525, doi:10.1175/JCLI-D-14-00236.1, 2014.
- Li, J. and Wang, J. X. L.: A modified zonal index and its physical sense, *Geophys. Res. Lett.*, 30(12), 1–4, doi:10.1029/2003GL017441, 2003.
- Liu, X., Xie, S., Boyle, J., Klein, S. A., Shi, X., Wang, Z., Lin, W., Ghan, S. J., Earle, M., Liu, P. S. K. and Zelenyuk, A.: Testing cloud microphysics parameterizations in NCAR CAM5 with ISDAC and M-PACE  
470 observations, *J. Geophys. Res. Atmos.*, 116(24), 1–18, doi:10.1029/2011JD015889, 2011.
- Loeb, N. G., Wielicki, B. A., Doelling, D. R., Smith, G. L., Keyes, D. F., Kato, S., Manalo-Smith, N. and Wong, T.: Toward optimal closure of the Earth’s top-of-atmosphere radiation budget, *J. Clim.*, 22(3), 748–766, doi:10.1175/2008JCLI2637.1, 2009.
- Lu, J. and Cai, M.: Seasonality of polar surface warming amplification in climate simulations, *Geophys. Res. Lett.*, 36(August), 1–6, doi:10.1029/2009GL040133, 2009.
- Madden, R. A. and Julian, P. R.: Detection of a 40–50 Day Oscillation in the Zonal Wind in the Tropical Pacific, *J. Atmos. Sci.*, 28(5), 702–708, doi:10.1175/1520-0469(1971)028<0702:DOADOI>2.0.CO;2, 1971.
- Morrison, H., Pinto, J. O., Curry, J. A. and McFarquhar, G. M.: Sensitivity of modeled arctic mixed-phase stratocumulus to cloud condensation and ice nuclei over regionally varying surface conditions, *J. Geophys. Res.*  
480 *Atmos.*, 113(5), 1–16, doi:10.1029/2007JD008729, 2008.
- Morrison, H., de Boer, G., Feingold, G., Harrington, J., Shupe, M. D. and Sulia, K.: Resilience of persistent Arctic mixed-phase clouds, *Nat. Geosci.*, 5(1), 11–17, doi:10.1038/ngeo1332, 2011.
- Neale, R. B., Gettelman, A., Park, S., Chen, C., Lauritzen, P. H., Williamson, D. L., Conley, A. J., Kinnison, D., Marsh, D., Smith, A. K., Vitt, F., Garcia, R., Lamarque, J., Mills, M., Tilmes, S., Morrison, H., Cameron-smith, P., Collins, W. D., Iacono, M. J., Easter, R. C., Liu, X., Ghan, S. J., Rasch, P. J. and Taylor, M. a: Description of the NCAR Community Atmosphere Model (CAM 5.0). NCAR Technical Notes., Tech. Note NCAR/TN-464+STR, 214, doi:10.5065/D6N877R0., 2012.
- Park, S.: A Unified Convection Scheme, UNICON. Part I. Formulation, *J. Atmos. Sci.*, (Lcl), 140808112307001, doi:10.1175/JAS-D-13-0234.1, 2014a.
- 490 Park, S.: A Unified Convection Scheme, UNICON. Part II. Simulation, *J. Atmos. Sci.*, (Lcl), 140808112307001, doi:10.1175/JAS-D-13-0234.1, 2014b.
- Park, S. and Bretherton, C. S.: The University of Washington shallow convection and moist turbulence schemes and their impact on climate simulations with the community atmosphere model, *J. Clim.*, 22(12), 3449–3469, doi:10.1175/2008JCLI2557.1, 2009.
- 495 Park, S., Bretherton, C. S. and Rasch, P. J.: Integrating Cloud Processes in the Community Atmosphere Model, Version 5, *J. Clim.*, 27(18), 6821–6856, doi:10.1175/JCLI-D-14-00087.1, 2014.
- Park, S., Baek, E.-H., Kim, B.-M. and Kim, S.-J.: Impact of detrained cumulus on climate simulated by the Community Atmosphere Model Version 5 with a unified convection scheme, *J. Adv. Model. Earth Syst.*, 6, 513–526, doi:10.1002/2016MS000877, 2017.
- 500 Park, S., Shin, J., Kim, S., Oh, E., and Kim, Y.: Global climate simulated by the Seoul National University Atmosphere Model Version 0 with a Unified Convection Scheme (SAM0-UNICON), *J. Clim.*, Accepted. 2019.
- Pithan, F. and Mauritsen, T.: Arctic amplification dominated by temperature feedbacks in contemporary climate models, *Nat. Geosci.*, 7(February), 2–5, doi:10.1038/NGEO2071, 2014.

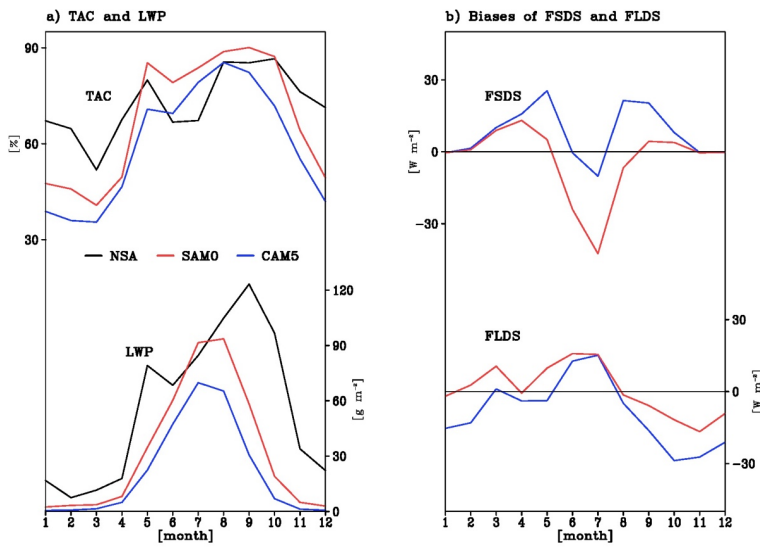
- 505 Pithan, F., Medeiros, B. and Mauritsen, T.: Mixed-phase clouds cause climate model biases in Arctic wintertime temperature inversions, *Clim. Dyn.*, 43(1–2), 289–303, doi:10.1007/s00382-013-1964-9, 2014.
- Prenni, A. J., DeMott, P. J., Kreidenweis, S. M., Harrington, J. Y., Avramov, A., Verlinde, J., Tjernström, M., Long, C. N. and Olsson, P. Q.: Can Ice-Nucleating Aerosols Affect Arctic Seasonal Climate?, *Bull. Am. Meteorol. Soc.*, 88(4), 541–550, doi:10.1175/BAMS-88-4-541, 2007.
- 510 Screen, J. A. and Simmonds, I.: The central role of diminishing sea ice in recent Arctic temperature amplification., *Nature*, 464(7293), 1334–1337, doi:10.1038/nature09051, 2010.
- Screen, J. A. and Simmonds, I.: Exploring links between Arctic amplification and mid-latitude weather, *Geophys. Res. Lett.*, 40(5), 959–964, doi:10.1002/grl.50174, 2013.
- Sedlar, J. and Tjernström, M.: Stratiform Cloud—Inversion Characterization During the Arctic Melt Season, *Boundary-Layer Meteorol.*, 132(3), 455–474, doi:10.1007/s10546-009-9407-1, 2009.
- 515 Serreze, M. C. and Barry, R. G.: Processes and impacts of Arctic amplification: A research synthesis, *Glob. Planet. Change*, 77(1–2), 85–96, doi:10.1016/j.gloplacha.2011.03.004, 2011.
- Shupe, M. D. and Intrieri, J. M.: Cloud radiative forcing of the Arctic surface: The influence of cloud properties, surface albedo, and solar zenith angle, *J. Clim.*, 17(3), 616–628, doi:10.1175/1520-0442(2004)017<0616:CRFOTA>2.0.CO;2, 2004.
- 520 Shupe, M. D., Kollias, P., Persson, P. O. G. and McFarquhar, G. M.: Vertical Motions in Arctic Mixed-Phase Stratiform Clouds, *J. Atmos. Sci.*, 65(4), 1304–1322, doi:10.1175/2007JAS2479.1, 2008.
- Shupe, M. D., Walden, V. P., Eloranta, E., Uttal, T., Campbell, J. R., Starkweather, S. M. and Shiobara, M.: Clouds at Arctic atmospheric observatories. Part I: Occurrence and macrophysical properties, *J. Appl. Meteorol. Climatol.*, 50(3), 626–644, doi:10.1175/2010JAMC2467.1, 2011.
- 525 Solomon, A., Shupe, M. D., Persson, P. O. G. and Morrison, H.: Moisture and dynamical interactions maintaining decoupled Arctic mixed-phase stratocumulus in the presence of a humidity inversion, *Atmos. Chem. Phys.*, 11(19), 10127–10148, doi:10.5194/acp-11-10127-2011, 2011.
- Taylor, K. E., Stouffer, R. J. and Meehl, G. A.: An overview of CMIP5 and the experiment design, *Bull. Am. Meteorol. Soc.*, 93(4), 485–498, doi:10.1175/BAMS-D-11-00094.1, 2012.
- 530 Walsh, J. E. and Chapman, W. L.: Arctic cloud-radiation-temperature associations in observational data and atmospheric reanalyses, *J. Clim.*, 11(11), 3030–3045, doi:10.1175/1520-0442(1998)011<3030:ACRTAI>2.0.CO;2, 1998.
- Wegener, A.: *Thermodynamik der Atmosphäre*, Barth., edited by J. A. Barth, Leipzig, Germany., 1911.
- 535 Wielicki, B. A., Barkstrom, B. R., Harrison, E. F., Lee, R. B., Smith, G. L. and Cooper, J. E.: Clouds and the Earth's Radiant Energy System (CERES): An Earth Observing System Experiment, *Bull. Am. Meteorol. Soc.*, 77(5), 853–868, doi:10.1175/1520-0477(1996)077<0853:CATERE>2.0.CO;2, 1996.
- Wu, Y. and Smith, K. L.: Response of Northern Hemisphere Midlatitude Circulation to Arctic Amplification in a Simple Atmospheric General Circulation Model, *J. Clim.*, 29(6), 2041–2058, doi:10.1175/JCLI-D-15-0602.1, 2016.
- 540 Xie, S., Liu, X., Zhao, C. and Zhang, Y.: Sensitivity of CAM5-Simulated Arctic Clouds and Radiation to Ice Nucleation Parameterization, *J. Clim.*, 26, 5981–5999, doi:10.1175/JCLI-D-12-00517.1, 2013.
- Zhang, G. J. and McFarlane, N. A.: Role of convective scale momentum transport in climate simulation, *J. Geophys. Res. Atmos.*, 100(D1), 1417–1426, doi:10.1029/94JD02519, 1995.

545 Xie, S., McCoy, R. B., Klein, S. a., Cederwall, R. T., Wiscombe, W. J., Clothiaux, E. E., Gaustad, K. L., Golaz, J. C., Hall, S. D., Jensen, M. P., Johnson, K. L., Lin, Y., Long, C. N., Mather, J. H., McCord, R. a., McFarlane, S. a., Palanisamy, G., Shi, Y. and Turner, D. D.: ARM climate modeling best estimate data: A new data product for climate studies, *Bull. Am. Meteorol. Soc.*, 91(1), 13–20, doi:10.1175/2009BAMS2891.1, 2010.

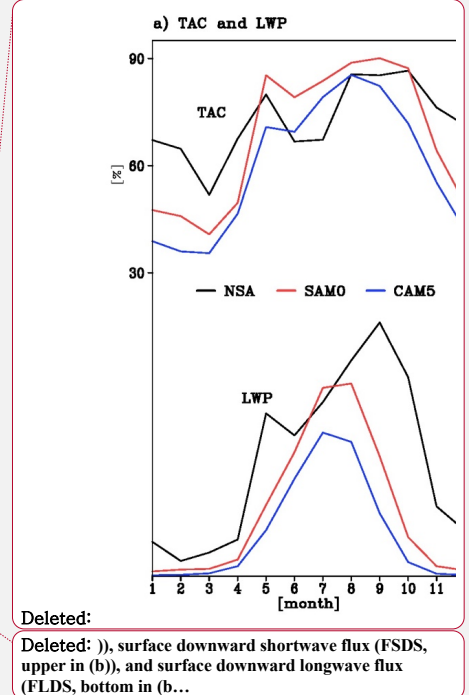
Figures



550 Figure 1: Annual cycles of (a) total cloud fraction (TCA) and (b) the height where the ratio of ice condensate mass to total condensate mass is 90 % (phase ratio, PR90) averaged over the Arctic area, north of 65° N from CALIPSO-GOCCP observations (black line), SAM0 (red line), and CAM5 (blue line). Dashed lines denote the standard deviation of each variable.



555  
560 Figure 2: Annual cycles of total cloud fraction (TAC, upper in (a)), liquid water path (LWP, bottom in (a)) from the climatology of ground-based cloud and radiation measurements at North Slope of Alaska (NSA) Barrow site (black line), SAM0 (red line), and CAM5 (blue line). Biases of surface downward shortwave flux (FSDS, upper in (b)) and surface downward longwave flux (FLDS, bottom in (b)) of SAM0 (red line), and CAM5 (blue line) against from the climatology of ground-based cloud and radiation measurements at North Slope of Alaska (NSA) Barrow site.



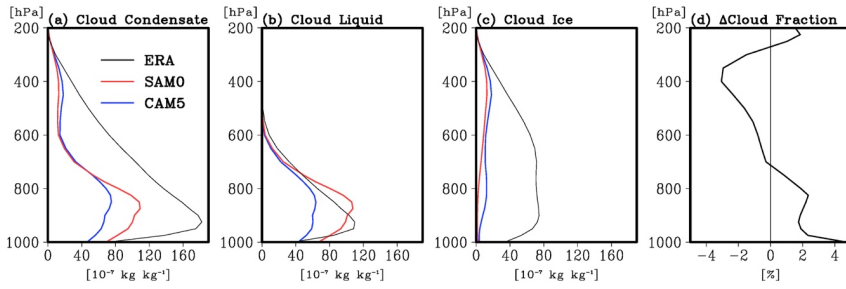


Figure 3: Annual-mean vertical profiles of grid-mean (a) cloud condensate mass (cloud liquid + cloud ice), (b) cloud liquid mass, and (c) cloud ice mass averaged over the Arctic area from ERA-interim (ERA, black lines), SAM0 (red lines) and CAM5 (blue lines), and (d) the difference of cloud fraction between SAM0 and CAM5.

Deleted:

Deleted: solid

Deleted: dotted

Deleted: )

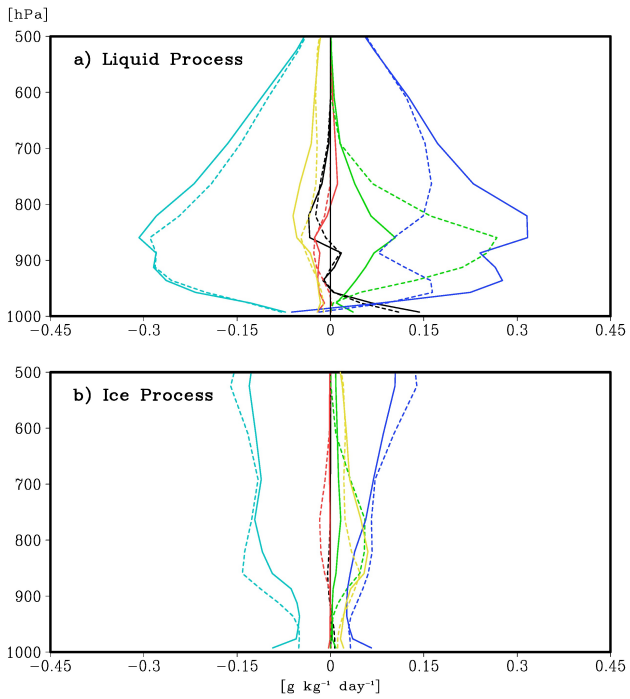
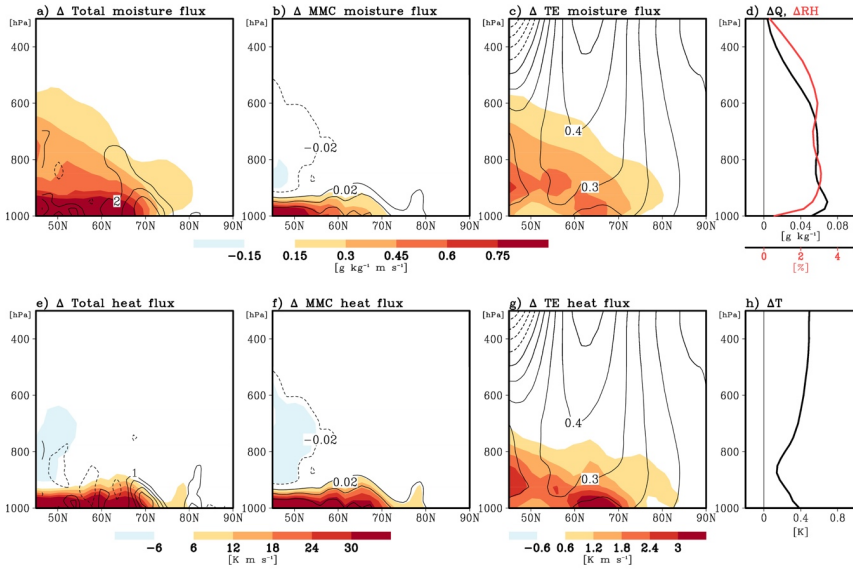


Figure 4: Annual-mean vertical profiles of the grid-mean tendencies of the (a) cloud liquid mass and (b) cloud ice mass induced by various moist physics processes from SAM0 (solid lines) and CAM5 (dotted lines). The processes shown are subgrid vertical transport by local symmetric turbulent eddies (PBL, black color), subgrid vertical transport by nonlocal asymmetric turbulent eddies (CON, red), convective detrainment (DET, green), net condensation of water vapor into cloud liquid and net deposition of water vapor into cloud liquid and ice (NCD, blue), precipitation-sedimentation fallout (PRS, cyan), and WBF conversion from cloud liquid mass to cloud ice mass (WBF, yellow).



585 Figure 5: Differences of zonal-mean meridional fluxes of (a, b, and c) moisture and (e, f, and g) heat by (a and e) total  
 processes (i.e., the transported sum by mean meridional circulation, stationary eddies, and transient eddies), (b and f)  
 mean meridional circulation (MMC), and (c and g) transient eddies (TE) between SAM0 and CAM5. Differences of the  
 590 annual-mean vertical profiles (d) water vapor ( $Q$ , black) and relative humidity (RH, red), and (h) air temperature ( $T$ )  
 averaged over the Arctic area between SAM0 and CAM5. The black lines in (a) and (e) denote the differences of zonal-  
 mean convergence of total moisture flux in  $10^{-7} \text{ g kg}^{-1} \text{ m s}^{-1}$  and total heat flux in  $10^{-5} \text{ K s}^{-1}$ . The black lines in (b) and  
 (f) denote the differences of zonal mean meridional wind in  $\text{m s}^{-1}$ . The black lines in (c) and (g) denote the differences  
 of zonal-mean zonal wind in  $\text{m s}^{-1}$  between SAM0 and CAM5, respectively. Most shaded areas exceed 95 % significance  
 level from the Student t-test.

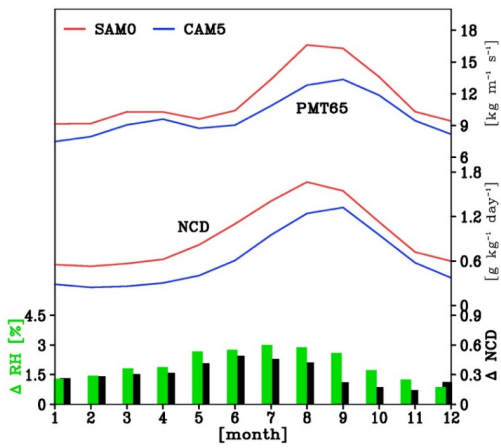


Figure 6: Annual cycles of vertically-integrated zonal-mean poleward moisture transport in  $\text{g kg}^{-1} \text{ m s}^{-1}$  at  $65^\circ \text{ N}$  (PMT65) and net condensation rate of water vapor into cloud liquid (NCD) in  $\text{g kg}^{-1} \text{ day}^{-1}$  averaged over the Arctic area from SAM0 (red line) and CAM5 (blue line).

Deleted: (NCD)

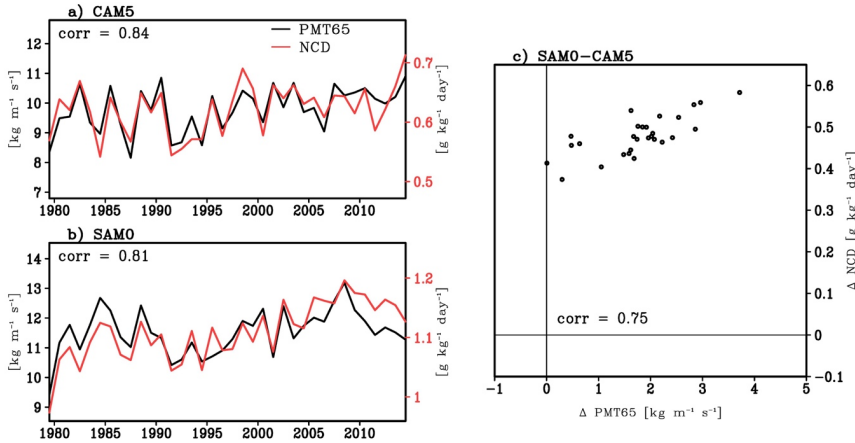


Figure 7: Interannual time series of the vertically-integrated annual-mean poleward moisture flux at  $65^\circ \text{ N}$  (PMT65, black line) and net condensation rate of water vapor into cloud liquid (NCD, red line) averaged over the Arctic area from (a) CAM5 and (b) SAM0, and (c) the scatter plot of the differences of annual-mean PMT65 and NCD between SAM0 and CAM5.

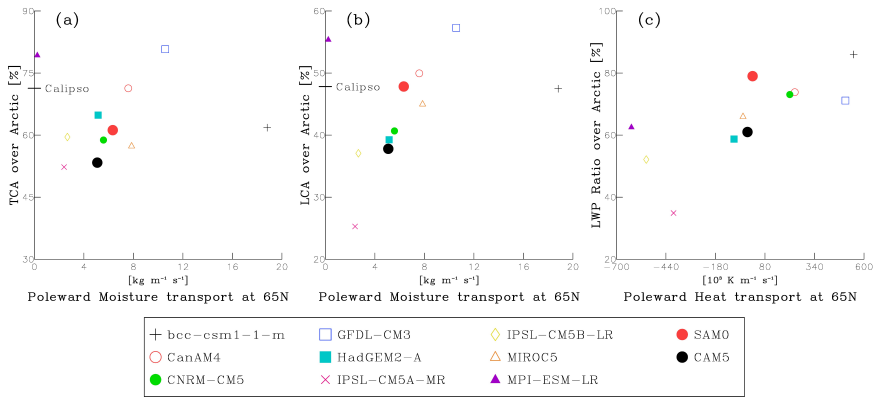


Figure 8: Scatter plots of the annual mean poleward fluxes of moisture and heat integrated over the vertical layers (1000–7000 hPa) at  $65^\circ \text{ N}$ , cloud fractions, and LWP ratio averaged over the Arctic area, obtained from various AMIP simulations of CMIP5 models, CAM5 and SAM0. The black lines in (a) and (b) denote the observed TCA and LCA, respectively, obtained from CALIPSO-GOCCP data.



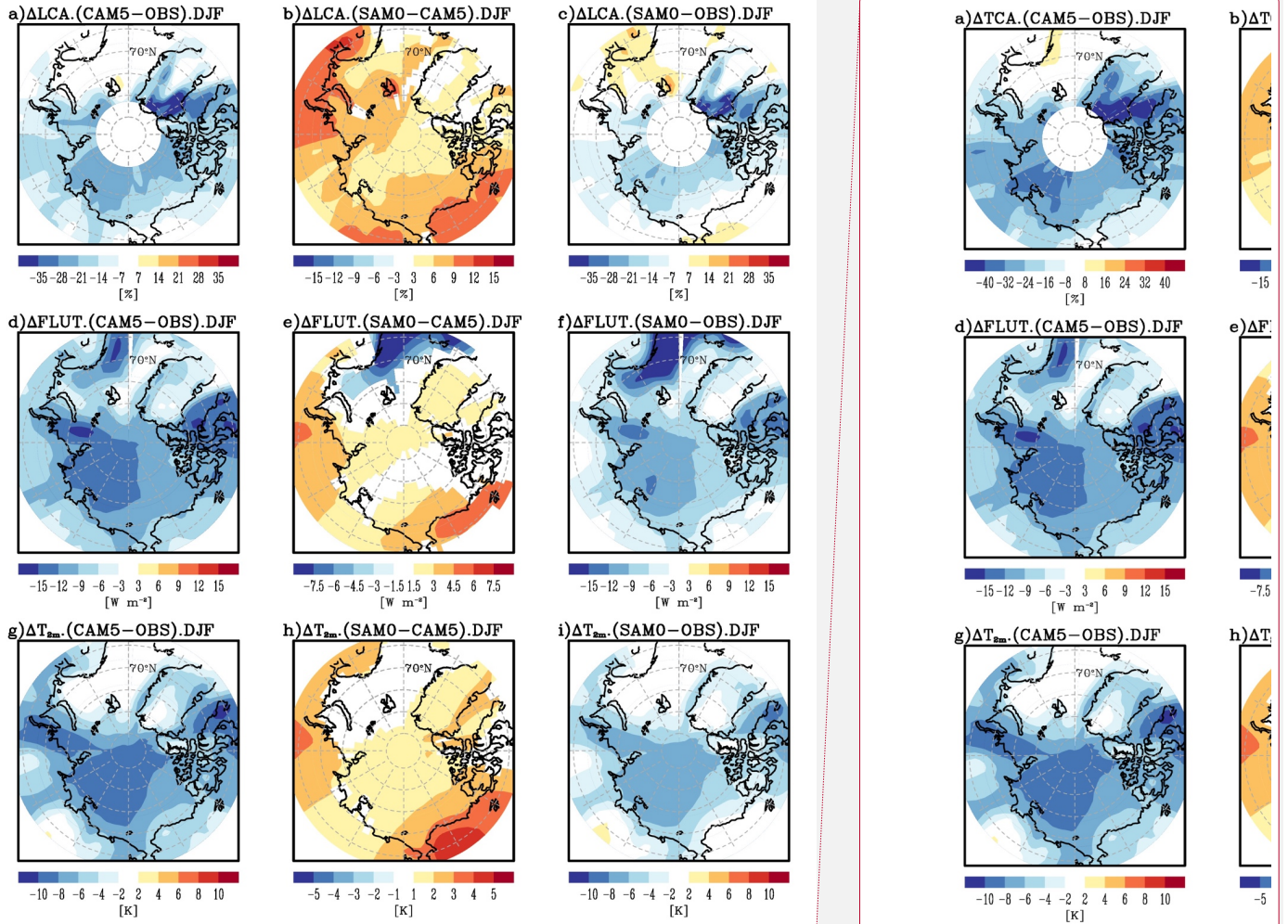
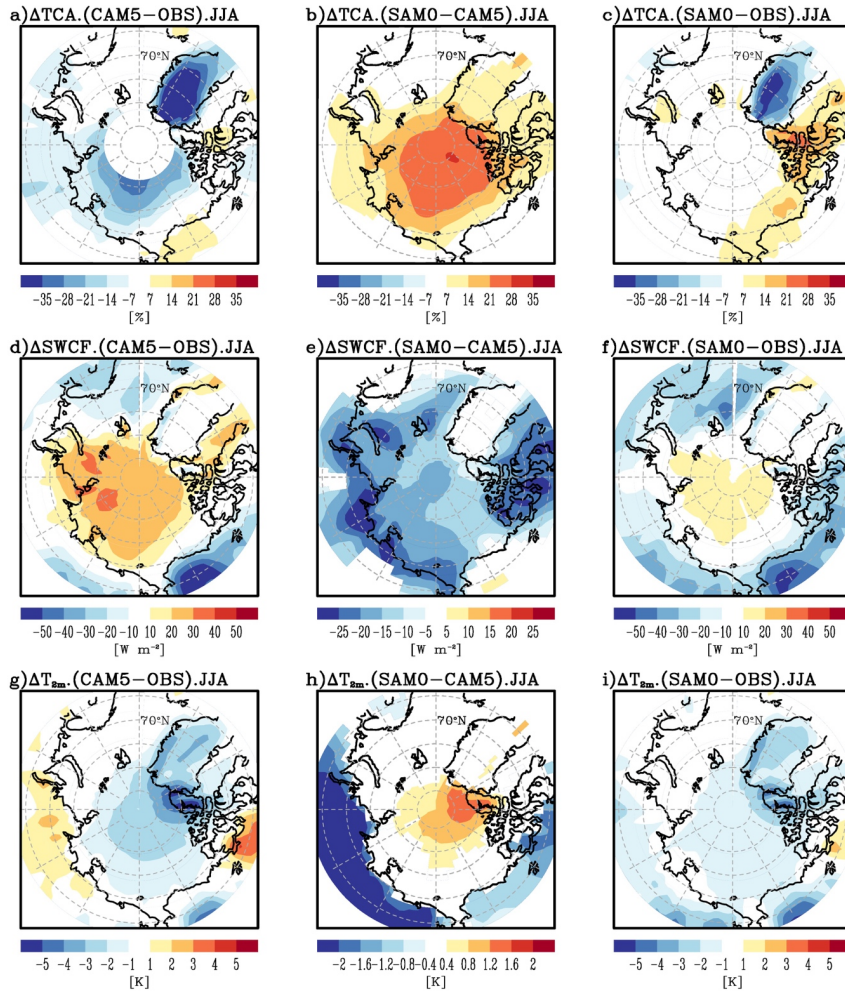
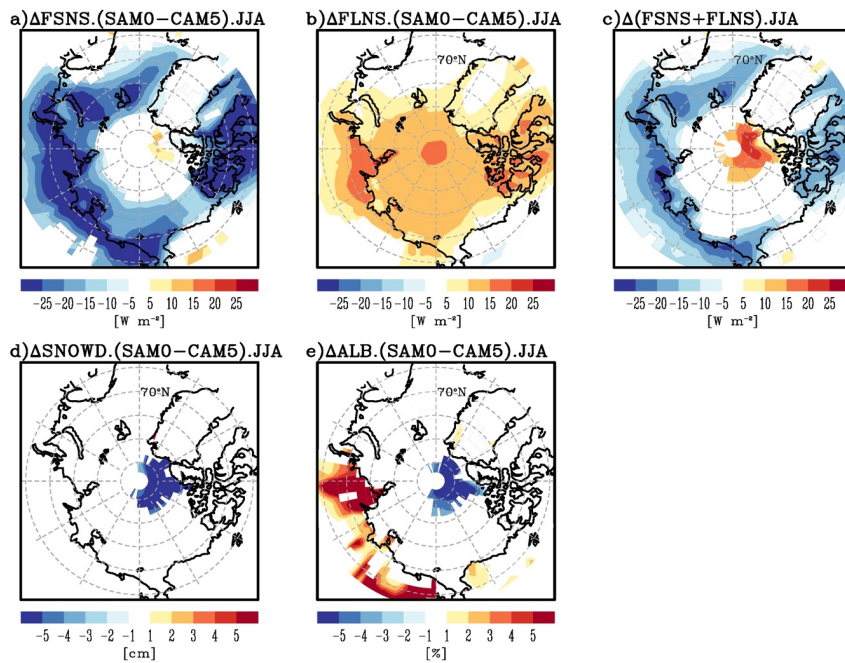


Figure 9: Biases of (upper) **Low cloud fraction (LCA)** against the CALIPSO-GOCCP observation, (middle) upward longwave (LW) radiative flux at TOA (FLUT) against the CERES-EBAF observation, and (lower) near-surface air temperature at a 2 m height ( $T_{2m}$ ) against the ERA-interim reanalysis during DJF obtained from (left) CAM5 and (right) SAM0, and (center) the differences of each variable between SAM0 and CAM5. Shaded areas in (b), (e), and (h) exceed 95 % significance level from the Student t-test.

Deleted: TCA



620 Figure 10: Identical with Fig. 8, except for **total cloud fraction (TCA) in the upper panel**, the shortwave cloud radiative forcing at TOA (SWCF) in the middle panel, and during JJA. Shaded areas in (b), (e), and (h) exceed 95% significance level from the Student t-test.



625 Figure 11: Differences of (a) net SW flux at the surface (FSNS), (b) net LW flux at the surface (FLNS), (c) sum of FSNS and FLNS, (d) snow depth (SNOWD), and (e) surface albedo (ALB) during JJA between SAM0 and CAM5. Shaded areas exceed 95 % significance level from the Student t-test.